Electrochemical and Solid-State Letters, **14** (7) B70-B73 (2011)
1099-0062/2011/14(7)/B70/4/$28.00 © The Electrochemical Society

One-Pot Synthesis of Platinum Nanoparticles Embedded on Reduced Graphene Oxide for Oxygen Reduction in Methanol Fuel Cells

Hyung-Wook Ha,[a] In Young Kim,[b] Seong-Ju Hwang,[b] and Rodney S. Ruoff[a,*,z]

[a]*Department of Mechanical Engineering and the Texas Materials Institute, The University of Texas at Austin, Austin, Texas 78712-0292, USA*
[b]*Center for Intelligent Nano-Bio Materials (CINBM), Department of Chemistry and Nano Sciences, College of Natural Sciences, Ewha Womans University, Seoul 120-750, Korea*

A simple approach has been developed for the synthesis of Pt nanoparticles with uniform diameters of approximately 2.9 nm supported on reduced graphene oxide (RG-O) platelets via a modified polyol method. Compared to Johnson Matthey (JM) Pt/C (75 wt % Pt) catalyst, the Pt/RG-O (70 wt % Pt) composite showed much higher electrochemical surface area, greater catalytic activity towards the oxygen reduction reaction (ORR), and significantly better single cell polarization performance. The maximum power density of the Pt/RG-O composite was about 128 mW cm^{-2}, an 11% greater than the JM Pt/C commercial catalyst.
 [DOI: 10.1149/1.3584092]

Manuscript submitted March 21, 2011; revised manuscript received April 7, 2011. Published April 27, 2011.

Direct methanol fuel cells (DMFCs)[1] are attractive alternatives to combustion engines in transportation applications for electrical power generation and are also regarded as promising future power sources, especially for mobile and portable applications due to their high energy density properties.[2] Platinum-based nanomaterials supported on carbon (e.g., Pt/C) are commonly employed electrocatalyst in DMFCs. However, unfortunately, there are serious barriers for commercialization of DMFCs technologies. One challenge is the parasitic methanol diffusion across the membrane, which brings out a significant degradation of cathode performance because of poisoning of the Pt catalyst and the occurrence of a mixed potential.[3,4] In order to further maximize the activity of Pt and minimize the amount of Pt, it is critical to load Pt nanostructures having high activity on the surface of supporting nanomaterials that are low cost, and have high surface area and good electrical conductivity. Recently, a polyol process using ethylene glycol (EG) as reducing agent[5–8] has been widely used. Compared with the traditional reduction method using impregnation by $NaBH_4$, the polyol process has demonstrated an enhanced control over the particle size and dispersion of the supported metal NPs; due to its rapid and homogenous *in situ* generation of reducing species, a uniform metal deposition on the carbon support is achieved. Graphene has attracted tremendous attention from both the experimental and theoretical scientific communities in recent years.[9,10] This two-dimensional (2-D) material composed of sp^2-bonded carbon atoms has a theoretical surface area of ~2630 $m^2\ g^{-1}$,[11] and with its high conductivity (10^3–10^4 S m^{-1}) suggest its use as a catalyst support.[12] Reduced graphene oxide (RG-O) has been studied as catalyst support.[13–18] Pt nanoparticles have previously been synthesized in the presence of graphene oxide (G-O) using polyol and microwave-assisted polyol methods,[7,8] However, the conditions used in these methods were not suitable for reducing the G-O. As such, most G-O-bound oxygen-containing functional groups remained. The catalyst support needs to have not only excellent dispersibility with large electrochemical surface area, but also high electronic conductivity.

We report a one step *in situ* modified polyol method to disperse Pt nanoparticles on reduced graphene oxide (RG-O), using H_2PtCl_6 as a Pt source, and EG and $NaBH_4$ as a reducing agent for Pt precursor and G-O, respectively. Well-dispersed Pt nanoparticles were thereby loaded onto the RG-O sheets. Transmission electron microscopy (TEM) and high-resolution TEM (HRTEM) as well as other analytical tools were used to determine the particle size and distribution of the Pt catalyst. The as-prepared Pt/RG-O composite exhibits significantly higher electrocatalytic activity than commercially available JM Pt/C catalyst toward methanol oxidation.

Experimental

Graphite oxide (GO) was synthesized by a modified Hummer's method.[19] Exfoliation of graphite oxide (GO) to graphene oxide (G-O) was achieved by ultrasonication of the dispersion in ethylene glycol (EG) for 1 h. Finally, a homogeneous G-O colloid (1 mg ml^{-1}) was obtained, as proven by observation of the Tyndall effect with a handheld laser pointer. In a typical run, Pt/RG-O with 70 wt % metal loading was prepared by the modified polyol process. 1.764 g of $H_2PtCl_6{\cdot}6H_2O$ (40% Pt based, Sigma-Aldrich) was first dissolved in 500 ml G-O colloid (1 mg ml^{-1}) in a three-necked flask, followed by addition of 1.12 g of NaOH under vigorous stirring at room temperature. The solution was continuously stirred and the reaction temperature was increased up to 120°C. When the reaction temperature reached 120°C, 20 ml of $NaBH_4$ dissolved in EG (20 mg ml^{-1}) was added dropwise and refluxed at 120°C for 1 h. After cooling to room temperature, the solution was added dropwise (thus, slowly) to 2 l of distilled water. The pH of this solution was adjusted to 7 by 0.1 M HCl (aq). The reduction product was separated by filtration and washed with large amounts of water several times to remove residual ions and then dried at 80°C in a vacuum oven for 12 h.

Cyclic voltammetry electrochemical measurements were carried out using a three-electrode cell configuration in 0.1 M H_2SO_4 at the rate of 20 mV s^{-1}. A glassy carbon (GC) electrode, platinum mesh electrode and Ag/AgCl system served as a *working*, *counter* and *reference* electrode, respectively. An electrical activity was assessed using a current density with respect to a unit weight. 16 mg of JM Pt/C and Pt/RG-O catalyst, 0.5 ml of 10 wt % Nafion solution, and 20 ml of distilled water was mixed to prepare a catalyst slurry. 3 μl of the catalyst slurry was doped on a 2 mm circular glassy carbon (GC) electrode. Linear sweep voltammetry was performed at 25.0°C in 0.1 M H_2SO_4 at a rotating rate of 1600 rpm with a glass carbon electrode at a scan rate of 10 mV/s.

Electrodes for a DMFC unit cell test were prepared using a spray method. TCP-H060 (Toray) and 24BC (SGL) were used as anode and cathode gas diffusion layers, respectively. Each catalyst was then suspended in a mixture of isopropyl alcohol and Nafion solution DE-1021 (Dupont, 10 wt % in water/aliphatic alcohols) and stirred to form a homogeneous slurry. The weight ratio of catalysts to dry Nafion was 75:25. The slurry was sprayed onto the prepared gas diffusion layer. Anode electrodes were prepared using commercially available PtRu (TEC81E81) catalysts (Tanaka, 81wt % PtRu). Cathode electrodes were prepared in the same way using a Pt/RG-O

* Electrochemical Society Active Member.
z E-mail: r.ruoff@mail.utexas.edu

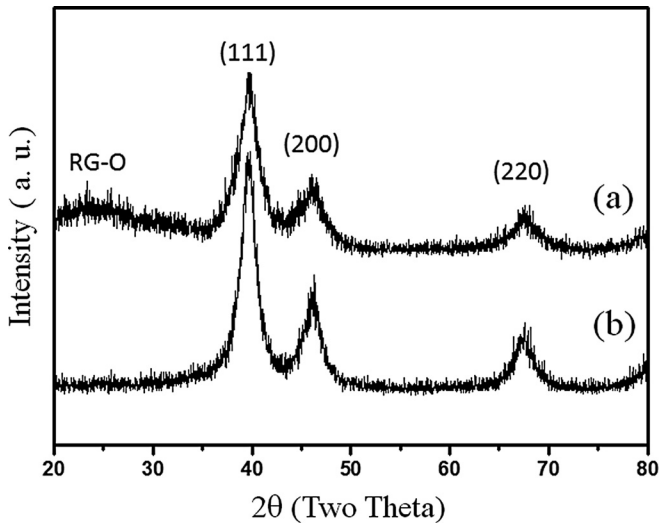

Figure 1. XRD patterns of (a) Pt/RG-O composite material and (b) commercially available Johnson Matthey (JM) Pt/C (75 wt % Pt) catalyst.

(70 wt % Pt) and JM Pt/C (75 wt % Pt) catalyst except with a weight ratio of catalysts to Nafion of 85:15. The catalyst loading at the anode and cathode were 1.8 and 1.2 mg_{Pt} cm^{-2}, respectively. The MEAs for a unit cell test were prepared by hot-pressing (150°C, 100 kgf cm^{-3} for 90 s) the anode and cathode layers onto both sides of a pretreated Nafion 115 membrane (Du-Pont). The geometric area of a unit cell was 4.84 cm^2. For unit cell operation, an aqueous solution of 1 M methanol was fed to the anode at a rate of 1 cc min^{-1}. The air was supplied to the cathode at flow rates of 100 cc min^{-1}. The operation of the unit cell was performed at ambient pressure, and the cell temperature was maintained at 60°C. The potential-current response of the unit cell was measured galvanostatically with an electronic loader. For the long-term stability test, the cell was measured at a constant current of 1 A using 1 M methanol (1 cc min^{-1}) and the air flow (100 cc min^{-1}) was *on* for 1770 s and *off* for 30 s at 60°C for 500 h.

The crystal structure of the Pt/RG-O composite was examined using high resolution-transmission electron microscopy (HR-TEM, Philips-CM200 microscope) and powder X-ray diffraction (XRD, Ni-filtered Cu Kα radiation with a graphite diffracted beam monochromator, 40 kV, 30 mA). X-ray photoelectron spectroscopy (XPS, Kratos AXIS Ultra DLD, Al Kα) was done on the Pt/RG-O composites. Raman measurements were made using a WiTec Alpha300 confocal Raman microscope with a 532 nm excitation source from a frequency-doubled Nd:Yag laser. Cyclic voltammetry electrochemical measurements were performed with an EG&G Park potentiostat/galvanostat Model M2273 (Princeton Applied research).

Results and Discussion

Figure 1 gives the XRD patterns of the Johnson Matthey commercial Pt nanoparticle (JM, Hispec 12100) and Pt/RG-O composite catalyst. XRD patterns showed a typical face-centered cubic (fcc) Pt lattice, and no impurity related peaks were observed. There were broad peaks centered at around 25° indicating an interlayer spacing of 0.355 nm, which is slightly higher than that of well-ordered graphite. The average Pt particle sizes calculated using the Scherrer equation were 4.1 and 2.9 nm for JM Pt/C and Pt/RG-O composite, respectively, suggesting larger Pt specific surface area in the RG-O composite. Transmission electron microscopy (TEM) images of the Pt/RG-O composite are shown in Fig. 2. Small Pt nanoparticles uniformly embedded on the surface of reduced graphene oxide sheets were observed. The HRTEM of Pt nanoparticles shows their size to be about 3 nm, relatively close to that obtained by the Scherrer analysis discussed above. The selected area electron diffraction (SAED) pattern (inset of Fig. 2c) shows a ring pattern of randomly overlapped and stacked RG-O sheets and sharp diffraction spots, from the crystalline Pt nanoparticles. The SAED pattern is indexed to the (111) and (220) reflections of face-centered cubic (fcc) platinum, respectively. The corresponding d-spacings are calculated to be 0.239 and 0.147 nm, respectively. Statistical analysis performed by measuring more than 100 Pt nanoparticles on TEM image. The histogram of the particle size distribution of Pt nanoparticles in the Pt/RG-O composite catalyst (Fig. 2d) shows a narrow distribution in the range of 2–3 nm, consistent with TEM data.

Figure 3A shows the Raman spectroscopy of GO and Pt/RG-O composite catalyst. The Raman spectra of GO shows a broad

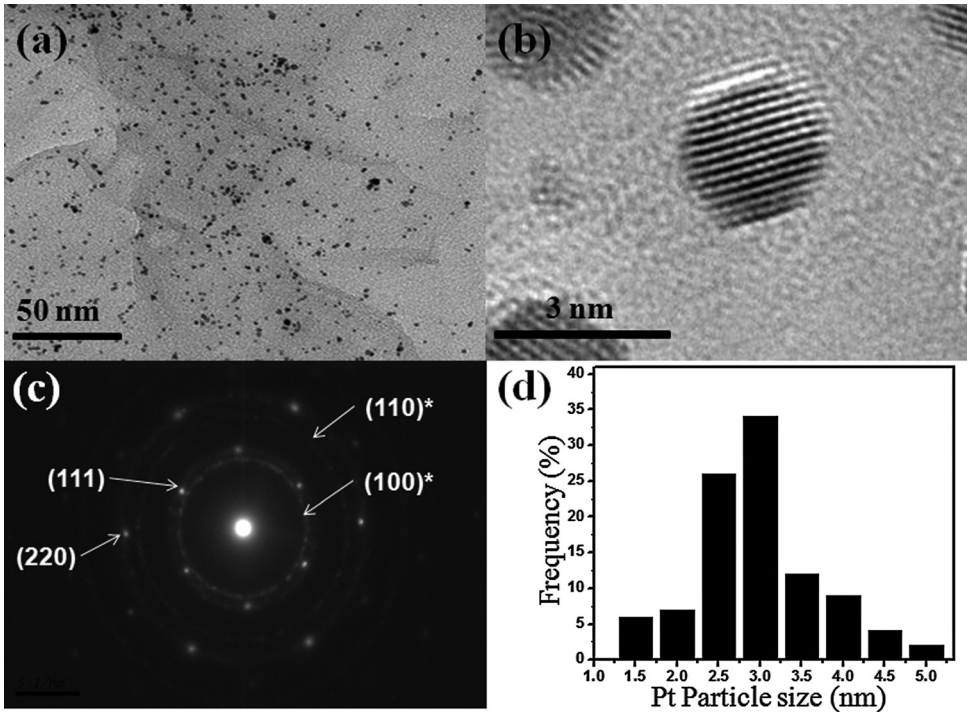

Figure 2. TEM image (a), HRTEM image (b) of Pt/RG-O composite, (c) SAED pattern of Pt/RG-O composite and (d) size distribution of Pt nanoparticles. The (hkl) of Pt and RG-O* are identified in the diffraction pattern in (c).

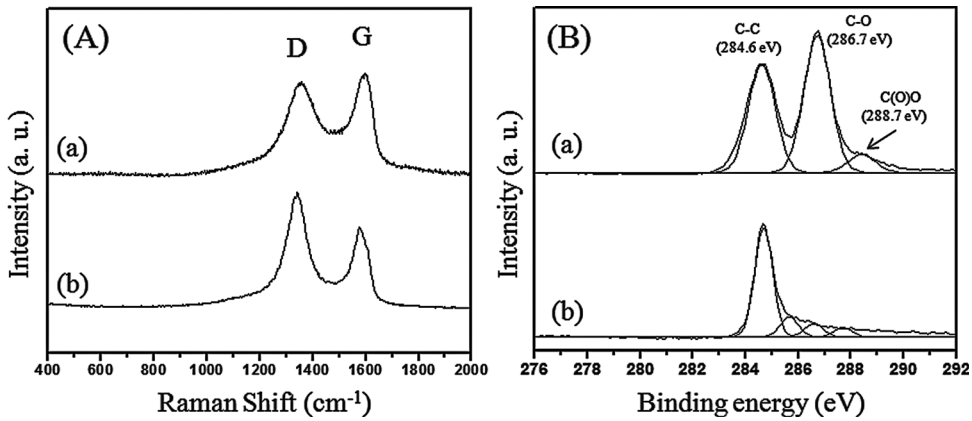

Figure 3. Raman spectra (A) and deconvoluted X-ray photoelectron spectroscopy (XPS) spectra (B) of (a) graphite oxide and (b) Pt/RG-O composite materials.

G-band at 1584 cm^{-1}, corresponding to the sp^2-hybridized carbon atoms in the hexagonal framework. The appearance of the prominent disorder mode at 1352 cm^{-1} is indicative of extensive oxidation of the graphite and the disruption of the sp^2-hybridized carbon atoms. As compared with GO, the D/G intensity ratio of Pt/RG-O composite increases, which has been said indicates a decrease in the average domain size of the sp^2-hybridized carbon atoms.[20] Figure 3B show X-ray photoelectron spectroscopy (XPS) spectra of GO and also of Pt/RG-O composite materials. As shown in Fig. 3B, the C1s spectrum of graphite oxide (GO) shows two main peaks centered at 284.6 and 286.7 eV. The peak at 284.6 eV is associated with the binding energy of sp^2 C-C bonds. The peak at 286.7 eV corresponds to C-O bonds in the epoxy/hydroxyl/carbonyl groups.[21] In comparison to the C1s spectrum of GO, that of the Pt/RG-O showed a strong reduction of the epoxy/hydroxyl/carbonyl groups (286.7 eV) peak, i.e., the oxygen-containing functional group peaks almost disappear. A combustion elemental analysis (measured by Atlantic Microlab Inc., Norcross, GA) gave C/O ratios of 1.02 for a GO powder sample and 4.67 for Pt/RG-O composite materials, respectively. The Raman, XPS, and elemental analysis results clearly demonstrate that these oxygen containing groups have been effectively removed by the modified polyol process.

The electrochemical behavior of Johnson Matthey commercial Pt nanoparticle (JM, Hispec 12100) and of the Pt/RG-O composite was studied in a 0.1 M H_2SO_4 solution using cyclic voltammograms (CV) with a sweep rate of 20 mV s^{-1}. Figure 4A shows the CV curves for the Pt/RG-O (Pt loading: 70 wt %) and JM Pt/C (Pt loading: 75 wt %). Based on the coulombic charge corresponding to the hydrogen adsorption/desorption features in the cyclic voltammogram, the calculated electrochemical surface area of Pt/RG-O (113 $m^2\ g_{Pt}^{-1}$) is approximately 3 times larger than that of previous Pt/RG-O composites prepared by polyol (36.27 $m^2\ g_{Pt}^{-1}$)[7] and microwave-assisted polyol methods (43.1 $m^2\ g_{Pt}^{-1}$),[8] and 1.5 times greater than that of the commercial JM Pt/C (74 $m^2\ g_{Pt}^{-1}$). This suggests that, in comparison, the Pt/RG-O composite prepared here has a much higher electrochemical activity for DMFC application.

Figure 4B compares oxygen reduction reaction (ORR) activities on Pt/RG-O and JM Pt/C catalysts from a rotating disc electrode (RDE) test in an O_2-saturated aqueous electrolyte solution containing 0.1 M H_2SO_4. It is found that the Pt/RG-O catalyst possesses

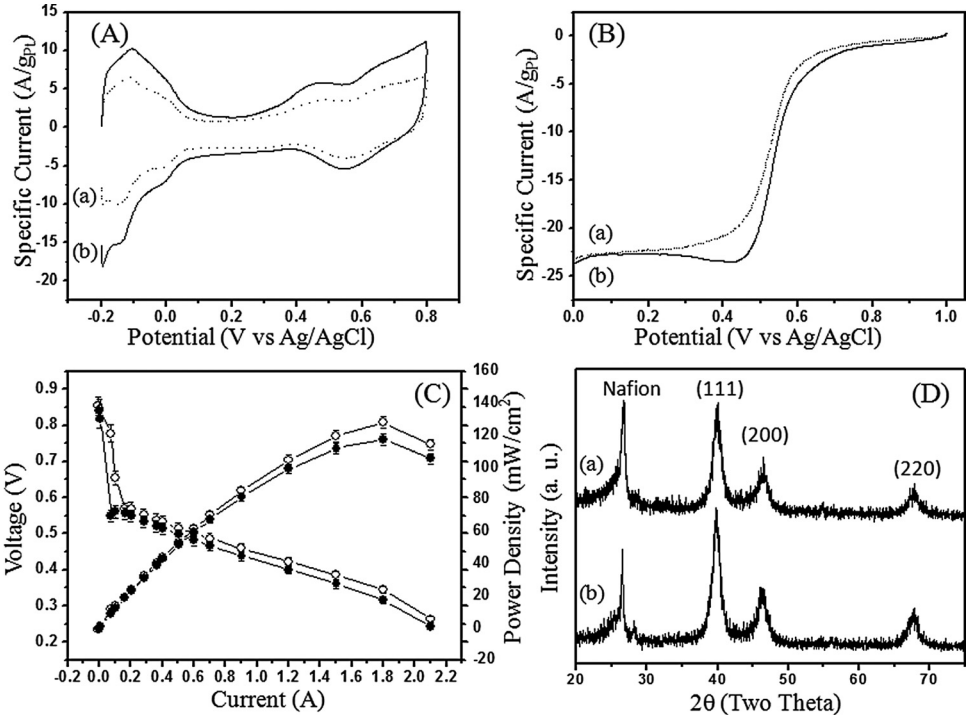

Figure 4. Cyclic voltammetry (A) and linear sweep voltammetry (B) of (a) JM Pt/C and (b) Pt/RG-O composite. Polarization and power density curves (C) of a direct methanol fuel cell employing JM Pt/C (closed circle) and Pt/RG-O (opened circle) as cathode catalyst, respectively. Anode fuel feeding, 1 M methanol at 1.0 cc min^{-1}; cell temperature, 60°C; Cathode fuel feeding, air at 100cc min^{-1}; 1.8 mg cm^{-2} metal loading of PtRu/C-81% (from Tanaka) anode catalyst; 1.2 mg cm^{-2} metal loading of Pt/RG-O-70% and Pt/C-75% (from JM) cathode catalyst. XRD patterns (D) of (a) Pt/RG-O composite catalyst and (b) JM Pt/C (75 wt % Pt) catalyst, each after 500 h long-term stability test.

much better ORR catalytic performance than the JM Pt/C catalyst. A positive shift of the onset potential at 0.6 V for oxygen reduction in the Pt/RG-O composite catalyst was observed as compared to the commercial JM Pt/C catalyst. At a given polarized potential of 0.6 V, where ORR is under kinetic control, the reduction current of ORR on Pt/RG-O composite and JM Pt/C are 4.94 and 3.17 A g_{Pt}^{-1}, respectively. The much larger electrochemical surface area of Pt/RG-O as compared to commercial JM Pt/C might lead to a much higher catalytic activity, and it facilitates the diffusion of O_2 on the surface of RG-O sheets to the Pt metal sites. These results indicate a significant improvement of electrocatalytic activity for ORR in Pt/RG-O composite.

Figure 4C shows the polarization performance of DMFCs at 60°C using Pt/RG-O and JM Pt/C cathode catalyst. As shown in Fig. 4C, the cell performance of Pt/RG-O cathode catalyst has much higher catalytic activity than the commercial JM Pt/C, which is likely due to the better supporting effect of the RG-O than the activated carbon of JM Pt/C. The current density at 0.4 V for the Pt/RG-O catalyst is 309 mA cm^{-2}, which is 25% higher than the value of 248 mA cm^{-2} for the JM Pt catalyst under the same test conditions. The maximum power density of Pt/RG-O is about 128 mW cm^{-2}, which is 11% larger than that of JM Pt/C (117.3 mW cm^{-2}). Figure 4D shows the XRD data of cathode catalysts after long-term stability testing. It has been found that the average particle sizes of JM Pt and Pt/RG-O have increased from 4.1 to 5.4 nm and 2.9 to 3.7 nm, respectively. The lower degree of agglomeration of the Pt particles should provide the reactants easier access to the catalytically active sites, thus improving the mass transport in the cell system. On the basis of the present findings, the present modified-polyol method appears to be superior to generate homogeneous nanosized Pt particles on the RG-O supports. The structure and physicochemical properties of carbon support may be more important in the final single-cell performance. Furthermore, the small size of the Pt particles enhanced the catalytic activity due to the larger electrochemical surface area.

Conclusions

In conclusion, a simple approach has been explored for synthesis of reduced graphene oxide supported Pt catalysts using a modified polyol method. This synthetic strategy achieves homogeneous deposition of Pt complex species on the surface of RG-O through *in situ* generation of reducing species by EG and $NaBH_4$ as a reducing agent. XPS and elemental analysis show that the graphene oxide has been reduced by this modified polyol method. In particular, the modified polyol strategy allows efficient synthesis of highly loaded Pt catalyst with small nanoparticle size and uniform particle dispersion. The Pt/RG-O composite catalyst not only outperforms the catalytic activity of the oxygen reduction reaction but also has enhanced fuel-cell polarization performance compared with the commercially available JM Pt/C catalyst. In addition, it has been found from the XRD analysis that the Pt particle size in the RG-O composite has increased less than that of the Pt particles in the commercial JM Pt catalyst, suggesting a higher catalytic activity during the long-term stability testing. The Pt/RG-O composites could be a promising catalyst for the DMFC application.

Acknowledgment

This work was supported by the National Science Foundation (DMR-0907324).

References

1. S. H. Joo, C. Pak, D. J. You, S.-A. Lee, H. I. Lee, J. M. Kim, H. Chang, and D. Seung, *Electrochim. Acta*, **52**,1618 (2006).
2. Z. Wen, J. Liu, and J. Li, *Adv. Mater.*, **20**, 743 (2008).
3. M.-H. Shao, K. Sasaki, and R. R. Adzic, *J. Am. Chem. Soc.*, **128**, 3526 (2006).
4. W. Yuan, K. Scott, and H. Cheng, *J. Power Sources*, **163**, 323 (2006).
5. W. Yu, W. Tu, and H. Liu, *Langmuir*, **15**, 6 (1998).
6. Z. Liu, J. Y. Lee, W. Chen, M. Han, and L. M. Gan, *Langmuir*, **20**, 181 (2003).
7. Y. Li, W. Gao, L. Ci, C. Wang, and P. M. Ajayan, *Carbon*, **48**, 1124 (2010).
8. S. Sharma, A. Ganguly, P. Papakonstantinou, X. Miao, M. Li, J. L. Hutchison, M. Delichatsios, and S. Ukleja, *J. Phys. Chem. C*, **114**, 19459 (2010).
9. Y. Zhu, S. Murali, W. Cai, X. Li, J. W. Suk, J. R. Potts, and R. S. Ruoff, *Adv. Mater.*, **22**, 3906.
10. A. K. Geim and K. S. Novoselov, *Nat. Mater.*, **6**, 183 (2007).
11. S. Stankovich, D. A. Dikin, G. H. B. Dommett, K. M. Kohlhaas, E. J. Zimney, E. A. Stach, R. D. Piner, S. T. Nguyen, and R. S. Ruoff, *Nature (London)*, **442**, 282 (2006).
12. S. Park and R. S. Ruoff, *Nat. Nanotechnol.*, **4**, 217 (2009).
13. B. Seger and P. V. Kamat, *J. Phys. Chem. C*, **113**, 7990 (2009).
14. R. Muszynski, B. Seger, and P. V. Kamat, *J. Phys. Chem. C*, **112**, 5263 (2008).
15. E. Yoo, T. Okata, T. Akita, M. Kohyama, J. Nakamura, and I. Honma, *Nano Lett.*, **9**, 2255 (2009).
16. X. Zhou, X. Huang, X. Qi, S. Wu, C. Xue, F. Y. C. Boey, Q. Yan, P. Chen, and H. Zhang, *J. Phys. Chem. C*, **113**, 10842 (2009).
17. S. Bong, Y.-R. Kim, I. Kim, S. Woo, S. Uhm, J. Lee, and H. Kim, *Electrochem. Commun.*, **12**, 129 (2010).
18. C. Xu, X. Wang, and J. Zhu, *J. Phys. Chem. C*, **112**, 19841 (2008).
19. W. S. Hummers and R. E. Offeman, *J. Am. Chem. Soc.*, **80**, 1339 (1958).
20. F. Tuinstra and J. L. Koenig, *J. Chem. Phys.*, **53**, 1126 (1970).
21. S. Stankovich, D. A. Dikin, R. D. Piner, K. A. Kohlhaas, A. Kleinhammes, Y. Jia, Y. Wu, S. T. Nguyen, and R. S. Ruoff, *Carbon*, **45**, 1558 (2007).